Berberine Attenuates Hepatic Steatosis and Enhances Energy Expenditure in Mice by Inducing Autophagy and Fibroblast Growth Factor 21

Yixuan Sun[1,2], Mingfeng Xia[1,2], Hongmei Yan[1,2], Yamei Han[3], Feifei Zhang[3], Zhimin Hu[3], Aoyuan Cui[3], Fengguang Ma[3], Zhengshuai Liu[3], Qi Gong[3], Xuqing Chen[3], Jing Gao[3], Hua Bian[1,2], Yi Tan[4,5], Yu Li[3]*, Xin Gao[1,2]*

[1]Department of Endocrinology and Metabolism, Zhongshan Hospital, Fudan University, Shanghai, China;
[2]Fudan Institute for Metabolic Diseases, Shanghai, China;
[3]CAS Key Laboratory of Nutrition and Metabolism, Institute for Nutritional Sciences, Shanghai Institutes for Biological Sciences, Chinese Academy of Sciences, University of Chinese Academy of Sciences, Shanghai 200031, China;
[4]Chinese-American Research Institute for Diabetic Complications, School of Pharmaceutical Science, Wenzhou Medical University, Wenzhou, Zhejiang 325035, China;
[5]Pediatric Research Institute at the Department of Pediatrics, Wendy L. Novak Diabetes Care Center, University of Louisville, Louisville, KY 40202, USA;

Supplemental Fig. 1

Sun Y, et al.

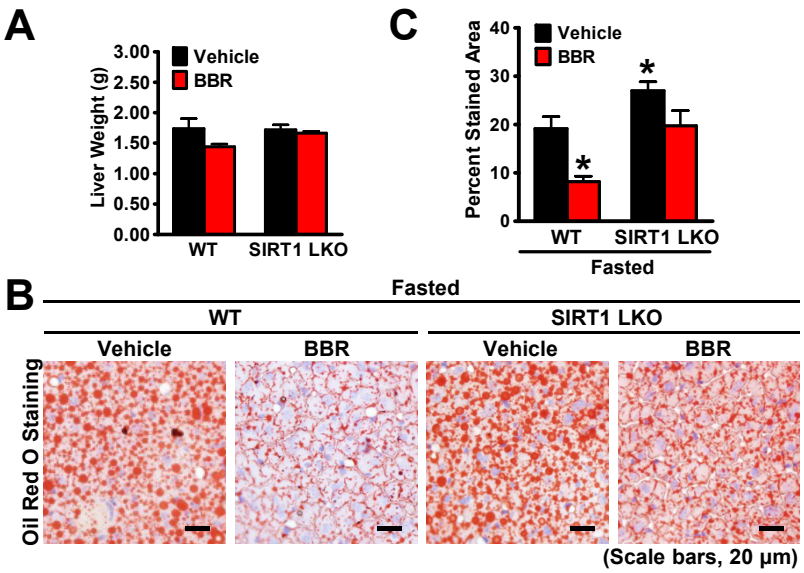

Supplemental Fig. 2

Sun Y, et al.

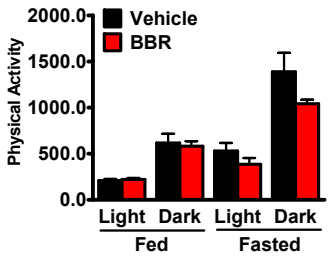

Supplemental Figure Legends

Fig.S1. The effects of hepatic SIRT1 deficiency on the liver weight or hepatic steatosis in HFHS diet-fed or fasted mice, respectively. (A) The liver weight of the mice was measured. Wild type (WT) and SIRT1 LKO male mice at sixteen-week-old were fed on a HFHS diet for 12 weeks, and then treated with berberine (5 mg/kg/day) or vehicle (PBS) by intraperitoneal injection once-daily for five weeks. The data are presented as the mean±SEM, n=6. (B-C) The beneficial effect of berberine on improving hepatic steatosis is compromised by hepatic specific deletion of SIRT1 in fasted mice. Male SIRT1 LKO or WT mice were treated without or with berberine (5 mg/kg/day) or vehicle (PBS) by intraperitoneal injection once-daily for four weeks, and then subjected to fasting for 24 hours (Fasted). Hepatic steatosis was assessed by Oil Red O staining (B) and quantification of Oil Red O stained areas (C). The data are presented as the mean±SEM，n=5, *P<0.05, versus WT mice treated with vehicle.

Fig.S2. Effects of berberine on physical activity in mice. Male C57BL/6 mice were treated with berberine (5 mg/kg/day) or vehicle (PBS) by intraperitoneal injection once-daily for four weeks. The physical activity were measured by comprehensive metabolic monitoring in mice over a 24-hour period with food and over a 24-hour fast, and normalized to lean body mass. The bar graph of physical activity is expressed as total counts measured by summing X and Y beam breaks over a 12-hour block of light and dark phases in the fed and fasted conditions. The data are presented as the mean±SEM, n=6.

Table S1. Quantitative RT-PCR primers

Gene	Species	Forward primer	Reverse primer

FGF21	mouse	CTGGGGGTCTACCAAGCATA	CACCCAGGATTTGAATGACC
UCP1	mouse	CACCTTCCCGCTGGACACT	CCCTAGGACACCTTTATACCTAATGG
DIO2	mouse	AGAGTGGAGGCGCATGCT	GGCATCTAGGAGGAAGCTGTTC
PRDM16	mouse	CAGCACGGTGAAGCCATTC	GCGTGCATCCGCTTGTG
β-actin	mouse	CCACAGCTGAGAGGGAAATC	AAGGAAGGCTGGAAAAGAGC
Atg5	human	TTTTGCACAAGAGGCTGGTC	GTGTTCCCTGCATTCTGATCC
β-actin	human	GATGAGATTGGCATGGCTTT	GTCACCTTCACCGTTCCAGT

Supplemental Experimental Procedures

Reagents and antibodies—Berberine (cat. B3251), chloroquine (cat. C6628), Oil Red O (cat. O0625), and palmitic acid (cat. P0500) were purchased from Sigma-Aldrich (St. Louis, MO). Rabbit polyclonal LC3 antibody (cat. 2775) and acetylated-lysine antibody (cat. 9441) were purchased from Cell Signaling Technology (Beverly, MA). Ex527 (cat. 2780) was from TOCRIS Bioscience (Bristol, UK). Mouse monoclonal β-actin (cat. sc-69879), horseradish peroxidase-conjugated anti-mouse and anti-rabbit secondary antibodies, and protein A/G PLUS-Agarose beads were obtained from Santa Cruz Biotechnology (Santa Cruz, CA).

Oil Red O staining—Oil Red O staining were performed as previously described(Chen et al., 2016). First, the fresh liver tissues were embedded in optimum cutting temperature compound (Tissue-Tek, Laborimpex), cut into 8-μm sections in a freezing microtome, and then mounted on a microscope slide. Second, the sections were fixed in formaldehyde vapors for 5 min at 4 °C, incubated in 60% isopropanol, and then stained in Oil Red O solution for 15 min. Third, the sections were incubated in 60% isopropanol, rinsed in distilled water twice, and then counterstained in hematoxylin solution for 1 min. After that, the sections were rinsed in distilled water for four times, mounted with aqueous

mounting medium, and then covered with a coverslip. Staining images were captured under a microscope (Olympus BX53). The relative stained areas of steatosis were quantified using ImageJ (National Institutes of Health, Bethesda, MD) and the results are presented as “Percent Stained Area” for unwanted sources of variation. Image J’s color deconvolution was performed to generate individual staining pattern of each image, as described previously (Ruifrok, 1997).

Measurement of plasma lipids, FGF21 and β-hydroxybutyrate—Infinity Triglycerides kit (cat. TR22421) and Total Cholesterol kit (cat. TR13421) were obtained from Stanbio Laboratory (Boerne, TX). The FGF21 enzyme-linked immunosorbent assay kits for mouse (cat. 32180) and human (cat. 31180) were obtained from Antibody and Immunoassay Services at the University of Hong Kong, China. The β-hydroxybutyrate LiquidColor Test kit (catalog no. 2440-58) was from Stanbio Laboratory (Boerne, TX).

Body Composition Analysis—Body composition was determined with the nuclear magnetic resonance system using a Body Composition Analyzer MiniQMR23-060H-I (Niumag, China). Body fat, lean mass, body fluids, and total body water were measured in live conscious mice with ad libitum access to chow as described previously(Li et al., 2014).

Energy Expenditure Measurements—Energy expenditure was assessed by indirect calorimetry measurements using Comprehensive Laboratory Animal Monitoring Systems (Columbus Instruments, Columbus, OH) as described previously(Li et al., 2014; Li, Wong, Walsh, Gao & Zang, 2013) in the Animal Core Facility at the Institute for Nutritional Sciences, Shanghai Institutes for Biological Sciences, Chinese Academy of Sciences. Individually housed mice were allowed free access to food and water, and acclimatized to respiratory chambers for 24 hours. The data for VO_2, VCO_2, and locomotor activity were recorded simultaneously over a 48-hour period, which was

divided into a 24-hour feed and a 24-hour fast. The VO_2 and VCO_2 rates were expressed as average values measured every 17 minutes over a 12-hour block in the light and dark cycles. The energy expenditure (kcal/kg/h) was calculated with the formula: $(3.815+1.232\times VCO_2/VO_2)\times VO_2\times 0.001$, and normalized to lean body mass as described previously(Hofmann et al., 2007; Li et al., 2014). Physical activity was measured by summing X and Y beam breaks over 12-hour intervals of the light and dark cycles in the same metabolic cage.

Plasmid construction and transfection—The lentiviral transfer plasmid pCDH-CMV-3xFLAG-PGC1α or pCDH-CMV-3xFLAG-Atg5 were constructed by cloning the cDNAs from mouse FLAG-PGC-1α(Li et al., 2008) or human FLAG-Atg5(Dong et al., 2013) plasmids into the SalI/NotI or NheI/BamHI sites of pCDH-CMV-3xFLAG vector(Zhang et al., 2016), respectively. The GFP-LC3 plasmid(Zhang et al., 2016) was constructed by cloning the cDNA of human LC3 into the SalI and NotI sites of pEGFP-C1 vector (Clontech). Transfection assays for plasmids were performed using Lipofectamine 2000 (Life Technologies) according to the manufacturer's protocol.

Lentiviral particles production—Lentiviral particles were generated as described previously(Gong et al., 2016). Briefly, HEK293T cells were cotransfected with 3 μg of lentiviral transfer plasmid pCDH-CMV-3xFLAG-PGC-1α or pCDH-CMV-3xFLAG-Atg5, along with 2 μg of packaging plasmids pMDLg/pRRE and pRSV-Rev (1:1 ratio), and 1 μg of envelope plasmid pMD2.G in a 6-cm plate using Lipofectamine 2000 (Life Technologies). Twelve hours post transfection, the media was changed, and cells were cultured in 5 ml fresh DMEM containing 10% fetal bovine serum, 100 units/ml penicillin, and 100 μg/ml streptomycin. Twenty four hours post incubation, the media that containing lentiviral particles was harvested and stored at 4 °C. The resulting cells were cultured in 5 ml fresh DMEM containing 10% fetal bovine serum, 100 units/ml penicillin, and 100 μg/ml

streptomycin, and then incubated for additional 24 hours. The media was then harvested and pooled with the media harvested in the previous day. The pooled media containing lentiviral particles was filtered through a 0.45 μm filter and then stored at 4 °C.

Lentiviral particles infection and selection—For lentivirus infection, cells were cultured to approximately 70% confluent. Then the media was changed, and cells were cultured in fresh media containing 8 μg/mL polybrene, followed by adding lentiviral particle solution to the media. Twenty-four hours post infection, the media was changed, and cells were selected and passaged under puromycin-containing media for 4-7 days. The resulting cells stably expressing mouse FLAG-tagged PGC-1α (St-FLAG-PGC-1α) or human FLAG-tagged Atg5 (St-FLAG-Atg5) were ready for further assays.

Immunoblotting analysis—Immunoblotting analysis was carried out as described previously(Chen et al., 2016; Gong et al., 2016; Li et al., 2014; Li et al., 2011). In brief, mouse liver tissues or cultured cells were homogenized and lysed at 4 °C in lysis buffer (50 mM Tris-HCl, pH 8.0, 1% (v/v) Nonidet P-40, 150 mM NaCl, 5 mM EDTA, 1 mM EGTA, 1 mM sodium orthovanadate, 10 mM sodium fluoride, 1 mM phenylmethylsulfonyl fluoride, 2 μg/ml aprotinin, 5 μg/ml leupeptin, and 1 μg/ml pepstatin). Cell lysates were centrifuged at 14,000 rpm for 10 min at 4 °C, and the resulting supernatant was used for immunoblotting analysis. Protein concentrations in cell lysates were measured using Bio-Rad Protein Assay Dye Reagent. For immunoblotting, 20–50 μg of protein were separated by 8-10% sodium dodecyl sulfate-polyacrylamide gel electrophoresis (SDS-PAGE), and then electrophoretically transferred to polyvinylidene difluoride (PVDF) membranes in a transfer buffer consisting of 25 mM Tris base, 190 mM glycine, and 20% methanol. The membranes were blocked with 5% non-fat milk in Tris-buffered saline with 0.1% Tween 20 (TBST) and incubated with specific antibodies, followed

by incubation with horseradish peroxidase-conjugated secondary antibodies. Immunoblots were visualized by LumiGLO chemiluminescence detection kit (Cell Signaling Technology). The intensity of bands was quantified using ImageJ (National Institutes of Health, Bethesda, MD).

Deacetylation assay—For Atg5 and PGC-1α deacetylation assays, FLAG-tagged Atg5 or FLAG-tagged PGC-1α protein in total cell lysates was immunoprecipitated with FLAG antibody and Protein A/G-Sepharose beads at 4°C overnight. The precipitates were washed three times with ice-cold lysis buffer. The acetylation of Atg5 or PGC-1α was subsequently detected by immunoblotting with an acetylated-lysine specific antibody.

Berberine and fatty acid preparation—Berberine and palmitate-BSA was prepared as described previously(Chang et al., 2010; Gong et al., 2016). Berberine stock was dissolved in PBS at 65 °C for 30 min to a concentration of 0.8 mg/ml for in vivo intraperitoneal injection, or in dimethylsulfoxide at a concentration of 20 mM followed by dilution to indicated concentration using cell culture medium for in vitro treatment, respectively, and then filtered through a 0.22 μm filter (Millipore), and stored at -80 °C. Palmitic acid was dissolved in 0.1 M NaOH solution at 90 °C for 10 min. Fatty acid-free BSA was dissolved in ddH_2O and incubated at 55 °C for 20 min. The palmitate was mixed with BSA to make 10 mM palmitate-BSA stock solution, and then filtered and stored at -20 °C. Control BSA solution was prepared by mixing 0.1 M NaOH with BSA.

Cell treatment—Cells were cultured in DMEM containing 5.5 mM D-glucose, 10% fetal bovine serum, 100 units/ml penicillin, and 100 μg/ml streptomycin, and incubated in a humidified atmosphere of 5% CO_2 at 37 °C and passaged every 2 days by trypsinization.

RNA isolation and quantitative RT-PCR analysis—Liver tissues were homogenized in TRIzol Reagent (Life Technologies) to extract total RNAs according to the manufacturer's protocol. Total

RNAs were then reversely transcribed to cDNA using SuperScript II reverse transcriptase (Life Technologies) and Oligo d (T). The resulting cDNA was subjected to real-time PCR with gene-specific primers in the presence of SYBR Green PCR master mix (Applied Biosystems) using StepOnePlus Real-Time PCR System (Applied Biosystems) as described previously(Li et al., 2011). The specificity of the PCR amplification was verified by analyzing the melting curve, and also by running products on an agarose gel. Data were analyzed using the ΔΔCT threshold cycle method. The mRNA levels of genes were normalized to those of β-actin and presented as relative levels to control for unwanted sources of variation. Primers were designed using Primer3 (v. 4.0).

Transmission electron microscopy—Transmission electron microscopy was performed using a modified method described previously(Song et al., 2015). First, liver tissues of mice were fixed in 2.5% glutaraldehyde buffer at 4 °C for overnight, and washed 3 times with phosphate-buffered saline (PBS). Then, tissues were further fixed in 1% osmic acid for 1.5 h, and then washed 3 times with PBS. Second, tissues were dehydrated by incubating in ascending series of ethanol from 30% to 100%, followed by incubating in acetone for 10 min. Third, tissues were infiltrated with a mixture of epon and acetone (1:1 ratio) for 1.5 h, incubated with epon at room temperature for overnight, followed by embedding in a capsule containing epon at 60 °C for 48 h. Fourth, tissue sections were cut (70 nm) using a Leica EM UC7 ultramicrotome and a Diatome Ultra35 diamond knife (DiATOME), mounted on 100 hex-mesh copper grids, and then counterstained with Reynold's lead citrate. Images were captured using a Tecnai G2 spirit (FEI, Czech) transmission electron microscope and images were captured using a Gatan Model 830 (Gatan, USA) camera with Digital Micrograph (Gatan, USA) software. The average numbers of autophagic vacuoles (AVs) were quantified from a

randomly selected pool of 5 fields of liver tissues under each condition, averaged, and expressed as the number of autophagic vacuoles per area for unwanted sources of variation.

Fluorescence microscopy—Fluorescence microscopies were performed to determine GFP-LC3 puncta in HeLa cells. Cells were seeded onto glass coverslips. Forty eight hours post transfection, cells were fixed in 4% paraformaldehyde and coverslips were mounted in ProLong Gold antifade reagent with DAPI (Life Technologies) to visualize the nuclei. Images were captured under a confocal microscope (Olympus FV1200).

Reference

Chang X, Yan H, Fei J, Jiang M, Zhu H, Lu D*, et al.* (2010). Berberine reduces methylation of the MTTP promoter and alleviates fatty liver induced by a high-fat diet in rats. Journal of Lipid Research 51**:** 2504-2515.

Chen X, Zhang F, Gong Q, Cui A, Zhuo S, Hu Z*, et al.* (2016). Hepatic ATF6 Increases Fatty Acid Oxidation to Attenuate Hepatic Steatosis in Mice Through Peroxisome Proliferator–Activated Receptor α. Diabetes 65**:** 1904-1915.

Ding WX, Li M, Chen X, Ni HM, Lin CW, Gao W*, et al.* (2010). Autophagy Reduces Acute Ethanol-Induced Hepatotoxicity and Steatosis in Mice. Gastroenterology 139**:** 1740-1752.

Dong S, Jia C, Zhang S, Fan G, Li Y, Shan P*, et al.* (2013). The REGγ Proteasome Regulates Hepatic Lipid Metabolism through Inhibition of Autophagy. Cell Metabolism 18**:** 380-391.

Gong Q, Hu Z, Zhang F, Cui A, Chen X, Jiang H*, et al.* (2016). Fibroblast growth factor 21 improves hepatic insulin sensitivity by inhibiting mammalian target of rapamycin complex 1 in mice. Hepatology 64**:** 425-438.

Hofmann SM, Zhou L, Perez-Tilve D, Greer T, Grant E, Wancata L*, et al.* (2007). Adipocyte LDL receptor–related protein–1 expression modulates postprandial lipid transport and glucose homeostasis in mice. The Journal of clinical investigation 117**:** 3271-3282.

Li S, Liu C, Li N, Hao T, Han T, Hill DE*, et al.* (2008). Genome-wide Coactivation Analysis of PGC-1α Identifies BAF60a as a Regulator of Hepatic Lipid Metabolism. Cell Metabolism 8**:** 105-117.

Li Y, Wong K, Giles A, Jiang J, Lee JW, Adams AC*, et al.* (2014). Hepatic SIRT1 Attenuates Hepatic Steatosis and Controls Energy Balance in Mice by Inducing Fibroblast Growth Factor 21. Gastroenterology 146**:** 539-549.e537.

Li Y, Wong K, Walsh K, Gao B, & Zang M (2013). Retinoic Acid Receptor β Stimulates Hepatic Induction of Fibroblast Growth Factor 21 to Promote Fatty Acid Oxidation and Control Whole-body Energy Homeostasis in Mice. Journal of Biological Chemistry 288**:** 10490-10504.

Li Y, Xu S, Mihaylova MM, Zheng B, Hou X, Jiang B*, et al.* (2011). AMPK Phosphorylates and Inhibits SREBP Activity to Attenuate Hepatic Steatosis and Atherosclerosis in Diet-Induced Insulin-Resistant Mice. Cell Metabolism 13**:** 376-388.

Ruifrok AC (1997). Quantification of immunohistochemical staining by color translation and automated thresholding. Analytical and quantitative cytology and histology 19**:** 107-113.

Song YM, Lee Y-h, Kim J-W, Ham D-S, Kang E-S, Cha BS*, et al.* (2015). Metformin alleviates hepatosteatosis by restoring SIRT1-mediated autophagy induction via an AMP-activated protein kinase-independent pathway. Autophagy 11**:** 46-59.

Zhang D, Wang W, Sun X, Xu D, Wang C, Zhang Q*, et al.* (2016). AMPK regulates autophagy by phosphorylating BECN1 at threonine 388. Autophagy 12**:** 1447-1459.